Available online at www.sciencedirect.com
SCIENCE DIRECT®
ELSEVIER
International Journal of Solids and Structures 43 (2006) 4631–4647
INTERNATIONAL JOURNAL OF SOLIDS and STRUCTURES
www.elsevier.com/locate/ijsolstr

Thin plate theory including surface effects

P. Lu [a,b,*], L.H. He [b], H.P. Lee [a,c], C. Lu [a]

[a] Institute of High Performance Computing, 1 Science Park Road, #01-01 The Capricorn, Science Park II, Singapore 117528, Singapore
[b] CAS Key Laboratory of Mechanical Behavior and Design of Materials, University of Science and Technology of China, Hefei, Anhui 230027, PR China
[c] Department of Mechanical Engineering, National University of Singapore, 9 Engineering Drive 1, Singapore 119620, Singapore

Received 18 March 2005
Available online 12 September 2005

Abstract

In the paper, a general thin plate theory including surface effects, which can be used for size-dependent static and dynamic analysis of plate-like thin film structures, is proposed. This theory is a modification and generalization of the thin plate model in [Lim, C.W., He, L.H., 2004. Size-dependent nonlinear response of thin elastic films with nano-scale thickness. Int. J. Mech. Sci. 46, 1715–1726]. With the general theory, the governing equations of Kirchoff and Mindlin plate models including surface effects are derived, respectively. Some numerical examples are provided to verify the validities of the theory.

Keywords: Surface elasticity; Thin film; Thin plate; Size-dependent; Surface effects

1. Introduction

Ultra-thin plate- or beam-like structures with submicron thicknesses have attracted much attention due to their potential as high sensitive, high frequency devices for applications in MEMS/NEMS (see, e.g., Evoy et al., 1999; Lavrik et al., 2004). Understanding mechanical properties of these elements are of fundamental concern in design and predicting performance of the devices. For structures with submicron sizes, due to the increasing surface-to-bulk ratio, surface effects are likely to be significant and can considerably

* Corresponding author. Address: Institute of High Performance Computing, 1 Science Park Road, #01-01 The Capricorn, Science Park II, Singapore 117528, Singapore.
E-mail address: lupin@ihpc.a-star.edu.sg (P. Lu).

0020-7683/$ - see front matter © 2005 Elsevier Ltd. All rights reserved.
doi:10.1016/j.ijsolstr.2005.07.036

modify macroscopic properties. Experiments (Wong et al., 1997; Cuenot et al., 2004), thermodynamic and atomistic simulations (Cammarate and Sieradzki, 1989; Sun and Zhang, 2003; Zhang and Sun, 2004; Zhou and Huang, 2004) indicate that effective elastic properties of nanobeams and nanoplates are strongly size-dependent. Despite molecular dynamics based methods have been increasingly applied to modeling and simulation of nanomaterials and nanostrctural elements, they are restricted by computational capacities. Even classical molecular dynamics computations are still limited to simulating on the order of 10^6–10^8 atoms for a few nanoseconds. For MEMS/NEMS structures and elements with at least one dimension in micro-range (micro/nanobeam, plates, thin film, etc.), modeling and simulation of their overall physical and mechanical properties and long time range dynamics analysis must be left to continuum methods. Therefore, size-independent classical plate theories, in which surface effects are ignored, can be modified accordingly for the modeling of ultra-thin plate-like structures.

It is known that surface of a solid is a region with its own atom arrangement and property differing from the bulk (Ibach, 1997; Muller and Saul, 2004). To incorporate the effects of the surface, Gurtin and Murdoch (1975a,b) modified the theory of classical mechanics by modeling the surface as a two-dimensional membrane with different material properties adhering to the underlying bulk material without slipping. The presence of surface stresses thus results in a set of non-classical boundary conditions, which present the surface tractions on the bulk substrate in terms of surface stresses and inertia. The non-classical boundary conditions, the surface stress–strain relations, and the equations of classical elasticity for bulk material together form a coupled system of field equations. Based on the approach, it is demonstrated that the surface effects can be interpreted and treated by additional size-dependent terms added to overall elastic moduli of considered structural elements (Miller and Shenoy, 2000). The surface elasticity theory by Gurtin and Murdoch (1975a,b) offers a continuum mechanics model to study mechanical behavior of material with surface effects, and have received increasing interests in more recent researches in studying some mechanical problems in structural elements with nanoscale dimensions (Murdoch, 1976; Gurtin and Murdoch, 1978; Miller and Shenoy, 2000; Shenoy, 2002; Sharma et al., 2003; Sharma and Ganti, 2004; He et al., 2004; Lim and He, 2004). This continuum mechanics approach relies significantly on reliable constitutive constants of the surface layer, which could be determined by experiments or atomistic computations. It is shown that with correctly choose surface elastic properties, the continuum model is generally found to agree well with atomistic simulations (Miller and Shenoy, 2000).

The purpose of this paper is to generalize the size-dependent thin plate model developed by Lim and He (2004) based on Gurtin and Murdoch's surface elasticity theory (1975a,b). Lim and He (2004) suggested a continuum model which can be applied to bending analysis of thin elastic film with nanoscale thickness. By reviewing the derivations of the model, it is found that the normal stress along the surface of bulk substrate is still ignored as treated in the classical plate theories, and therefore, some of the surface equilibrium relations in Gurtin and Murdoch (1975a,b) cannot be satisfied. This simplification is accurate enough for the problems with relatively large-scale sizes. If the thickness of studied film is reduced to its critical length scale, this treatment may induce some errors, especially for nanosized problems.

To take into account the equilibrium of surface, the normal stress inside and on the surface of bulk substrate is introduced in the present work. Since the plate structures are thin, the normal stress along the thickness inside the bulk material can be assumed properly (linear assumption in the paper), and satisfies the constitutive relations on the surface. The general governing equations of the thin plate including surface effects can be derived by integrating the constitutive equations of bulk material through the thickness and replacing bulk stress components on the surface by the surface stress components through the equilibrium relations between the surface and the bulk materials. With proper assumptions for displacement components, a specific plate theory can be further obtained. As applications, the basic equations for Kirchhoff and Mindlin plate theories including surface effects are provided, and some examples are illustrated.

2. Governing equations

Consider a thin plate structure with thickness h. A Cartesian coordinate system x_i $(i = 1,2,3)$ is introduced so that the axes x_1 and x_2 are coordinates lying in the mid-plane of the plate, and the upper and lower surfaces S^+ and S^- of the plate are defined by $x_3 = \pm h/2$, respectively.

The equations of motion for the body of the plate are given by

$$\sigma_{ij,j} + f_i = \rho \ddot{u}_i, \tag{1}$$

where σ_{ij} and u_i denote, respectively, stress and displacement, f_i the body forces, and ρ the density. The surface stresses on the surfaces S^+ and S^- of the plate are denoted by $\tau^+_{i\alpha}$ and $\tau^-_{i\alpha}$, respectively, and satisfied the equilibrium relations (Gurtin and Murdoch, 1975a, 1978)

$$\begin{aligned} &\tau^+_{\beta i,\beta} - \sigma^+_{i3} = \rho^+_0 \ddot{u}^+_i, \quad \text{at } x_3 = h/2, \\ &\tau^-_{\beta i,\beta} + \sigma^-_{i3} = \rho^-_0 \ddot{u}^-_i, \quad \text{at } x_3 = -h/2, \end{aligned} \tag{2}$$

where $\sigma^+_{i3} = \sigma_{i3}(x_\beta, h/2; t)$ and $\sigma^-_{i3} = \sigma_{i3}(x_\beta, -h/2; t)$ are bulk stresses at $x_3 = \pm h/2$, respectively, $u^+_i = u_i(x_\beta, h/2; t)$ and $u^-_i = u_i(x_\beta, -h/2; t)$ are displacements at $x_3 = \pm h/2$, respectively, and $\rho^\pm_0$ are the surface densities of the surface layers S^+ and S^-, respectively. In (1) and (2) and throughout the paper, Latin subscripts range from the values 1 to 3, while Greek subscripts range over 1 and 2.

Since the thickness of the plate is very small compared to the other two dimensions, the governing equations (1) can be integrated through the thickness to obtain the global plate equations. To this end, define resultant forces N_{ij} and resultant moments M_{ij} as

$$N_{ij} = \int_{-h/2}^{h/2} \sigma_{ij}\, \mathrm{d}x_3, \qquad M_{ij} = \int_{-h/2}^{h/2} \sigma_{ij} x_3\, \mathrm{d}x_3. \tag{3}$$

Multiplying Eq. (1) by $\mathrm{d}x_3$, and integrating through the thickness, we have

$$N_{i\alpha,\alpha} + \sigma^+_{i3} - \sigma^-_{i3} + p_i = \int_{-h/2}^{h/2} \rho \ddot{u}_i\, \mathrm{d}x_3, \tag{4}$$

where $p_i = \int_{-h/2}^{h/2} f_i\, \mathrm{d}x_3$. Furthermore, multiplying Eq. (1) by $x_3\, \mathrm{d}x_3$, and integrating through the thickness, we have

$$M_{i\beta,\beta} - N_{i3} + \frac{h}{2}(\sigma^+_{i3} + \sigma^-_{i3}) + r_i = \int_{-h/2}^{h/2} \rho \ddot{u}_i x_3\, \mathrm{d}x_3, \tag{5}$$

where $r_i = \int_{-h/2}^{h/2} f_i x_3\, \mathrm{d}x_3$. Since the equation with $i = 3$ in (5) has no physical application, it is omitted in the rest derivations.

Substituting the surface equilibrium relations (2) into (4) and (5), the governing equations of the plate including the surface effects are obtained as

$$\begin{aligned} &N_{i\beta,\beta} + \tau^+_{\beta i,\beta} + \tau^-_{\beta i,\beta} + p_i = \int_{-h/2}^{h/2} \rho \ddot{u}_i\, \mathrm{d}x_3 + \rho^+_0 \ddot{u}^+_i + \rho^-_0 \ddot{u}^-_i, \\ &M_{\alpha\beta,\beta} + \frac{h}{2}(\tau^+_{\beta\alpha,\beta} - \tau^-_{\beta\alpha,\beta}) - N_{\alpha 3} + r_\alpha = \int_{-h/2}^{h/2} \rho \ddot{u}_\alpha x_3\, \mathrm{d}x_3 + \frac{h}{2}(\rho^+_0 \ddot{u}^+_\alpha - \rho^-_0 \ddot{u}^-_\alpha). \end{aligned} \tag{6}$$

If the surface stresses are neglected, Eqs. (6) are reduced to classical global plate equations.

Define the generalized resultant forces and resultant moments as

$$N^*_{i\alpha} = N_{i\alpha} + \tau^+_{\alpha i} + \tau^-_{\alpha i}, \qquad M^*_{\alpha\beta} = M_{\alpha\beta} + \frac{h}{2}(\tau^+_{\beta\alpha} - \tau^-_{\beta\alpha}), \tag{7}$$

the governing equations (6) can be further written as

$$\begin{aligned} N^{*}_{i\beta,\beta} + p_i &= \int_{-h/2}^{h/2} \rho \ddot{u}_i \, \mathrm{d}x_3 + \rho_0^{+}\ddot{u}_i^{+} + \rho_0^{-}\ddot{u}_i^{-}, \\ M^{*}_{\alpha\beta,\beta} - N_{\alpha 3} + r_\alpha &= \int_{-h/2}^{h/2} \rho \ddot{u}_\alpha x_3 \, \mathrm{d}x_3 + \frac{h}{2}(\rho_0^{+}\ddot{u}_\alpha^{+} - \rho_0^{-}\ddot{u}_\alpha^{-}). \end{aligned} \tag{8}$$

Eqs. (8) are general governing equations of plate including surface effects. For different plate theories, the related equations of motion can be obtained by substituting the assumed displacement components u_i into (8).

3. Constitutive relations

Assume that both the bulk and surfaces of the plate are homogeneous and isotropic, the constitutive relations of the bulk materials is expressed by

$$\sigma_{ij} = \lambda \varepsilon_{kk}\delta_{ij} + 2\mu\varepsilon_{ij}, \tag{9}$$

where λ and μ are Lamé constants, δ_{ij} the Kronecker delta, and ε_{ij} the strain components given by

$$\varepsilon_{ij} = \tfrac{1}{2}(u_{i,j} + u_{j,i}). \tag{10}$$

Since the plate is thin, the stress component σ_{33} are small comparing to the in plane stress components $\sigma_{\alpha\beta}$, which is simply assumed to be zero in the classical plate theories. However, the surface conditions (2) will not be satisfied with the assumption. To improve the weakness, it is assumed here that the stress component σ_{33} varies linearly through the thickness and satisfies the balance conditions on the surfaces. With the assumption, σ_{33} can be written as

$$\begin{aligned} \sigma_{33} &= \frac{1}{2}(\sigma_{33}^{+} + \sigma_{33}^{-}) + \frac{1}{h}(\sigma_{33}^{+} - \sigma_{33}^{-})x_3 \\ &= \frac{1}{2}(\tau^{+}_{\beta 3,\beta} - \tau^{-}_{\beta 3,\beta} - \rho_0^{+}\ddot{u}_3^{+} + \rho_0^{-}\ddot{u}_3^{-}) + \frac{1}{h}(\tau^{+}_{\beta 3,\beta} + \tau^{-}_{\beta 3,\beta} - \rho_0^{+}\ddot{u}_3^{+} - \rho_0^{-}\ddot{u}_3^{-})x_3. \end{aligned} \tag{11}$$

It is noted that the relation (11) is also suitable for the materials with anisotropic properties. The stress–strain relations (9) can then be simplified as

$$\sigma_{i\beta} = \frac{E}{1+\nu}\left(\varepsilon_{i\beta} + \frac{\nu}{1-\nu}\varepsilon_{\gamma\gamma}\delta_{i\beta}\right) + \frac{\nu}{1-\nu}\sigma_{33}\delta_{i\beta}, \tag{12}$$

where E is Young's modulus, and ν Poisson's ratio.

The constitutive relations of the surface layers S^{+} and S^{-} as given by Gurtin and Murdoch (1975a,b, 1978) can be expressed as

$$\tau^{\pm}_{\alpha\beta} = \tau_0^{\pm}\delta_{\alpha\beta} + (\mu_0^{\pm} - \tau_0^{\pm})(u^{\pm}_{\alpha,\beta} + u^{\pm}_{\beta,\alpha}) + (\lambda_0^{\pm} + \tau_0^{\pm})u^{\pm}_{\gamma,\gamma}\delta_{\alpha\beta} + \tau_0^{\pm}u^{\pm}_{\alpha,\beta}, \qquad \tau^{\pm}_{\alpha 3} = \tau_0^{\pm}u^{\pm}_{3,\alpha}, \tag{13}$$

where $\tau_0^{\pm}$ are residual surface tensions under unconstrained conditions, $\lambda_0^{\pm}$ and $\mu_0^{\pm}$ the surface Lamé constants, on the surfaces S^{+} and S^{-}, respectively. If the top and bottom layers have same material properties, the stress–strain relations (13) reduce to

$$\tau^{\pm}_{\alpha\beta} = \tau_0\delta_{\alpha\beta} + (\mu_0 - \tau_0)(u^{\pm}_{\alpha,\beta} + u^{\pm}_{\beta,\alpha}) + (\lambda_0 + \tau_0)u^{\pm}_{\gamma,\gamma}\delta_{\alpha\beta} + \tau_0 u^{\pm}_{\alpha,\beta}, \qquad \tau^{\pm}_{\alpha 3} = \tau_0 u^{\pm}_{3,\alpha}, \tag{14}$$

and the stress component σ_{33} in (11) is reduced to

$$\sigma_{33} = \frac{1}{2}\left[\tau^+_{\beta 3,\beta} - \tau^-_{\beta 3,\beta} - \rho_0(\ddot{u}^+_3 - \ddot{u}^-_3)\right] + \frac{1}{h}\left[\tau^+_{\beta 3,\beta} + \tau^-_{\beta 3,\beta} - \rho_0(\ddot{u}^+_3 + \ddot{u}^-_3)\right]x_3. \tag{15}$$

4. Basic equations for two plate theories

The most commonly used thin plate theories include Kirchhoff plate theory and Mindlin plate theory. The basic equations of these two plate theories are obtained in this section based on the discussions above.

4.1. Kirchhoff plate theory

In Kirchhoff plate theory, the displacement components are assumed to have the form

$$u_\alpha = u^0_\alpha - x_3 u^0_{3,\alpha}, \qquad u_3 = u^0_3, \tag{16}$$

where $u^0_i = u^0_i(x_\beta; t)$ is the displacement components of the mid-plane at time t.

Substituting (16) into (8), and defining

$$I = \int_{-h/2}^{h/2} \rho \, \mathrm{d}x_3 = \rho h, \qquad J = \int_{-h/2}^{h/2} \rho x_3^2 \, \mathrm{d}x_3 = \frac{\rho h^3}{12}, \tag{17}$$

one has the equations $M^*_{\alpha\beta,\beta} - N_{\alpha 3} + r_\alpha = -\left[J + h^2(\rho^+_0 + \rho^-_0)/4\right]\ddot{u}^0_{3,\alpha} + \left[h(\rho^+_0 - \rho^-_0)/2\right]\ddot{u}^0_\alpha$ and $N^*_{i\beta,\beta} + p_i = (I + \rho^+_0 + \rho^-_0)\ddot{u}^0_i - [h(\rho^+_0 - \rho^-_0)/2]\ddot{u}^0_{3,\alpha}\delta_{i\alpha}$, which can be further simplified as

$$\begin{aligned} N^*_{\alpha\beta,\beta} + p_\alpha &= (I + \rho^+_0 + \rho^-_0)\ddot{u}^0_\alpha - \frac{h}{2}(\rho^+_0 - \rho^-_0)\ddot{u}^0_{3,\alpha}, \\ M^*_{\alpha\beta,\alpha\beta} + \tau^+_{\beta 3,\beta} + \tau^-_{\beta 3,\beta} + r_{\alpha,\alpha} + p_3 &= (I + \rho^+_0 + \rho^-_0)\ddot{u}^0_3 - \left[J + \frac{h^2}{4}(\rho^+_0 + \rho^-_0)\right]\ddot{u}^0_{3,\alpha\alpha} + \frac{h}{2}(\rho^+_0 - \rho^-_0)\ddot{u}^0_{\alpha,\alpha}. \end{aligned} \tag{18}$$

By comparing (18) with the equations of motion of thin plate obtained by Lim and He (2004), it is found that the terms $(\tau^+_{\beta 3,\beta} + \tau^-_{\beta 3,\beta})$ relating surface stresses in the last equation of (18) were missing in their derivations.

The strain components for the plate theory can be obtained by substituting (16) into (10) as

$$\varepsilon_{\alpha\beta} = \varepsilon^0_{\alpha\beta} - x_3 u^0_{3,\alpha\beta}, \qquad \varepsilon_{3\alpha} = 0, \tag{19}$$

with

$$\varepsilon^0_{\alpha\beta} = \frac{1}{2}(u^0_{\alpha,\beta} + u^0_{\beta,\alpha}). \tag{20}$$

The resultant forces $N^*_{\alpha\beta}$ and the resultant moments $M^*_{\alpha\beta}$ for the Kirchhoff plate theory can be obtained by substituting (16) and (19) into (12)–(15), and then into (3) and (7). If the top and bottom surface layers have considered having the same material properties, the resultant forces can be obtained as

$$\begin{aligned} N^*_{\alpha\beta} &= 2\tau_0(\delta_{\alpha\beta} + u^0_{\alpha,\beta}) + \frac{Eh}{1-\nu^2}\left[(1-\nu)\left(1 + 2\frac{l_2 - l_1}{h}\right)\varepsilon^0_{\alpha\beta} + \nu\left(1 + \frac{l_3}{h}\right)\varepsilon^0_{\gamma\gamma}\delta_{\alpha\beta}\right], \\ M^*_{\alpha\beta} &= -\frac{Eh^3}{12(1-\nu^2)}\left[(1-\nu)\left(1 + 3\frac{l_2}{h}\right)u^0_{3,\alpha\beta} + \nu\left(1 + \frac{3l_3 - l_1}{h}\right)u^0_{3,\gamma\gamma}\delta_{\alpha\beta}\right] - \frac{h^2\nu}{6(1-\nu)}\rho_0\ddot{u}^0_3\delta_{\alpha\beta}, \end{aligned} \tag{21}$$

where

$$l_1 = \frac{2(1+\nu)\tau_0}{E}, \qquad l_2 = \frac{2(1+\nu)\mu_0}{E}, \qquad l_3 = \frac{2(1-\nu^2)(\lambda_0+\tau_0)}{E\nu}, \tag{22}$$

are material characteristic lengths indicating surface effect. The equations of motion (18) are thus expressed by displacements as

$$\begin{aligned}
&2\tau_0 u^0_{\alpha,\beta\beta} + \frac{Eh}{1-\nu^2}\left[\frac{1-\nu}{2}\left(1+2\frac{l_2-l_1}{h}\right)(u^0_{\alpha,\beta\beta}+u^0_{\beta,\alpha\beta}) + \nu\left(1+\frac{l_3}{h}\right)u^0_{\gamma,\gamma\beta}\delta_{\alpha\beta}\right] + p_\alpha = (I+2\rho_0)\ddot{u}^0_\alpha,\\
&2\tau_0 u^0_{3,\alpha\alpha} - \frac{Eh^3}{12(1-\nu^2)}\left[(1-\nu)\left(1+3\frac{l_2}{h}\right)u^0_{3,\alpha\beta\alpha\beta} + \nu\left(1+\frac{3l_3-l_1}{h}\right)u^0_{3,\gamma\gamma\alpha\beta}\delta_{\alpha\beta}\right] + r_{\alpha,\alpha} + p_3\\
&\quad = (I+2\rho_0)\ddot{u}^0_3 - \left[J+\frac{h^2}{6}\frac{3-4\nu}{1-\nu}\rho_0\right]\ddot{u}^0_{3,\alpha\alpha}.
\end{aligned} \tag{23}$$

The plate thickness dependent terms with l_i in (21) and (23) can be regarded as modifications of overall elastic moduli by considering surface effects.

4.2. Mindlin plate theory

In Mindlin plate theory, the displacement components are assumed to have the form

$$u_\alpha = u^0_\alpha + x_3\psi_\alpha, \qquad u_3 = u^0_3, \tag{24}$$

where $\psi_\alpha = \psi_\alpha(x_\beta;t)$ are independent variables. By substituting (24) into (8), the motion equations of Mindlin plate theory including surface effect can be written as

$$\begin{aligned}
&N^*_{i\beta,\beta} + p_i = (I+\rho_0^+ + \rho_0^-)\ddot{u}^0_i + \frac{h}{2}(\rho_0^+ - \rho_0^-)\ddot{\psi}_\alpha\delta_{i\alpha},\\
&M^*_{\alpha\beta,\beta} - N_{\alpha 3} + r_\alpha = \left[J + \frac{h^2}{4}(\rho_0^+ + \rho_0^-)\right]\ddot{\psi}^+_\alpha\frac{h}{2}(\rho_0^+ - \rho_0^-)\ddot{u}^0_\alpha.
\end{aligned} \tag{25}$$

The strain components for the plate theory can be obtained by substituting (24) into (10) as

$$\varepsilon_{\alpha\beta} = \varepsilon^0_{\alpha\beta} + x_3\varepsilon^1_{\alpha\beta}, \qquad \varepsilon_{3\alpha} = \frac{1}{2}(u^0_{3,\alpha} + \psi_\alpha), \tag{26}$$

with

$$\varepsilon^0_{\alpha\beta} = \frac{1}{2}(u^0_{\alpha,\beta} + u^0_{\beta,\alpha}), \qquad \varepsilon^1_{\alpha\beta} = \frac{1}{2}(\psi_{\alpha,\beta} + \psi_{\beta,\alpha}). \tag{27}$$

The resultant forces $N^*_{i\beta}$ and resultant moments $M^*_{\alpha\beta}$ for the Mindlin plate theory can be obtained by substituting (24) and (26) into (12)–(15), and then into (3) and (7). If the top and bottom surface layers have considered having the same material properties, the resultant forces can be obtained as

$$\begin{aligned}
N^*_{\alpha\beta} &= 2\tau_0(\delta_{\alpha\beta} + u^0_{\alpha,\beta}) + \frac{Eh}{1-\nu^2}\left[(1-\nu)\left(1+2\frac{l_2-l_1}{h}\right)\varepsilon^0_{\alpha\beta} + \nu\left(1+\frac{l_3}{h}\right)\varepsilon^0_{\gamma\gamma}\delta_{\alpha\beta}\right],\\
N^*_{3\beta} &= \frac{Eh}{2(1+\nu)}\left[\left(1+2\frac{l_1}{h}\right)u^0_{3,\beta} + \psi_\beta\right],\\
M^*_{\alpha\beta} &= \frac{Eh^3}{12(1-\nu^2)}\left\{(1-\nu)\left[\left(1+6\frac{l_2-l_1}{h}\right)\varepsilon^1_{\alpha\beta} + 3\frac{l_1}{h}\psi_{\alpha,\beta}\right] + \nu\left[\left(1+3\frac{l_3}{h}\right)\varepsilon^1_{\gamma\gamma} + \frac{l_1}{h}u^0_{3,\gamma\gamma}\right]\delta_{\alpha\beta}\right\} - \frac{h^2\nu}{6(1-\nu)}\rho_0\ddot{u}^0_3\delta_{\alpha\beta},
\end{aligned} \tag{28}$$

where l_1 to l_3 are same as those defined in (22).

The equations of motion (25) are thus expressed by displacements as

$$
\begin{aligned}
&2\tau_0 u^0_{\alpha,\beta\beta} + \frac{Eh}{1-\nu^2}\left[\frac{1-\nu}{2}\left(1+2\frac{l_2-l_1}{h}\right)(u^0_{\alpha,\beta\beta}+u^0_{\beta,\alpha\beta}) + \nu\left(1+\frac{l_3}{h}\right)u^0_{\gamma,\gamma\beta}\delta_{\alpha\beta}\right] + p_\alpha = (I+2\rho_0)\ddot{u}^0_\alpha,\\
&\frac{Eh}{2(1+\nu)}\left[\left(1+2\frac{l_1}{h}\right)u^0_{3,\beta\beta}+\psi_{\beta,\beta}\right] + p_3 = (I+2\rho_0)\ddot{u}^0_3,\\
&\frac{Eh^3}{12(1-\nu^2)}\left\{\frac{1-\nu}{2}\left[\left(1+6\frac{l_2-l_1}{h}\right)(\psi_{\alpha,\beta\beta}+\psi_{\beta,\alpha\beta})+3\frac{l_1}{h}\psi_{\alpha,\beta\beta}\right] + \nu\left[\left(1+3\frac{l_3}{h}\right)\psi_{\gamma,\gamma}+\frac{l_1}{h}u^0_{3,\gamma\gamma\beta}\right]\delta_{\alpha\beta}\right\}\\
&\quad -\frac{Eh}{2(1+\nu)}\left[u^0_{3,\beta}+\psi_\beta\right] + r_\alpha = \left(J+\frac{h^2}{2}\rho_0\right)\ddot{\psi}^+_\alpha - \frac{h^2\nu}{6(1-\nu)}\rho_0\ddot{u}^0_{3,\alpha}.
\end{aligned}
\tag{29}
$$

5. Examples—Cylindrical bending of plates

As examples, we consider applications of the theories derived above to simply supported cylindrical bending and vibration of an infinitely wide thin plate with finite length l, in which the displacements, strains and stresses depend on coordinate x_1 only. In the examples, numerical illustrations are produced based on calculated results from two sets of material parameters given in Gurtin and Murdoch (1978):

$$
E = 5.625\times10^{10}\ \mathrm{N/m^2},\quad \nu = 0.25,\quad \rho = 3\times10^3\ \mathrm{kg/m^3},\quad \lambda_0 = 7\times10^3\ \mathrm{N/m},\quad \mu_0 = 8\times10^3\ \mathrm{N/m},\\
\tau_0 = 110\ \mathrm{N/m},\quad \rho_0 = 7\times10^{-4}\ \mathrm{kg/m^2},
$$

for Material I, and

$$
E = 17.73\times10^{10}\ \mathrm{N/m^2},\quad \nu = 0.27,\quad \rho = 7\times10^3\ \mathrm{kg/m^3},\quad \lambda_0 = -8\ \mathrm{N/m},\quad \mu_0 = 2.5\ \mathrm{N/m},\\
\tau_0 = 1.7\ \mathrm{N/m},\quad \rho_0 = 7\times10^{-6}\ \mathrm{kg/m^2},
$$

for Material II.

5.1. Solutions with Kirchhoff theory

In cylindrical bending, the displacements in (16) rely on x_1 only, i.e. $u^0_i = u^0_i(x_1;t)$. Therefore, the nonzero resultant forces and moments are reduced to

$$
\begin{aligned}
&N^*_{11} = 2\tau_0 + \frac{Eh}{1-\nu^2}\left(1+\frac{\eta_1}{h}\right)u^0_{1,1},\qquad N^*_{21} = \frac{Eh}{2(1+\nu)}\left(1+\frac{2l_2}{h}\right)u^0_{2,1},\\
&M^*_{11} = -\frac{Eh^3}{12(1-\nu^2)}\left(1+\frac{\eta_2}{h}\right)u^0_{3,11} - \frac{\nu h^2}{6(1-\nu)}\rho_0\ddot{u}^0_3,
\end{aligned}
\tag{30}
$$

where

$$
\eta_1 = (1-\nu)(2l_2-l_1)+\nu l_3,\qquad \eta_2 = 3(1-\nu)l_2+\nu(3l_3-l_1),
\tag{31}
$$

and the equations of motion (23) are reduced to

$$\begin{aligned}
&\frac{Eh}{1-\nu^2}\left(1+\frac{\eta_1}{h}\right)u^0_{1,11}+p_1=(I+2\rho_0)\ddot{u}^0_1,\\
&\frac{Eh}{2(1+\nu)}\left(1+\frac{2l_2}{h}\right)u^0_{2,11}+p_2=(I+2\rho_0)\ddot{u}^0_2,\\
&2\tau_0 u^0_{3,11}-\frac{Eh^3}{12(1-\nu^2)}\left(1+\frac{\eta_2}{h}\right)u^0_{3,1111}+r_{1,1}+p_3=(I+2\rho_0)\ddot{u}^0_3-\left(J+\frac{h^2}{6}\frac{3-4\nu}{1-\nu}\rho_0\right)\ddot{u}^0_{3,11}.
\end{aligned} \tag{32}$$

The simply supported boundary conditions along edges $x_1=0$ and l are defined by

$$u^0_3=0,\qquad N^*_{11}=N^*_{21}=M^*_{11}=0. \tag{33}$$

5.1.1. Static bending

For static cylindrical bending, the displacements satisfying the boundary conditions (33) can be written as

$$u^0_\alpha=U^*_{\alpha K}\cos q_n x_1,\qquad u^0_3=U^*_{3K}\sin q_n x_1, \tag{34}$$

where

$$q_n=n\pi/l, \tag{35}$$

with n being a positive integral, and $U^*_{\alpha K}$ and U^*_{3K} indicate maximal values of displacement components under Kirchhoff theory.

Further assuming that the plate is subjected to sinusoidal loading $p_3=P_3\sin q_n x_1$ only, and $p_1=p_2=r_1=0$. The following relations for the static cylindrical bending can thus be obtained by substituting (34) and loading conditions in (32) as

$$U^*_{1K}=U^*_{2K}=0,\qquad U^*_{3K}=P_3\Big/\left\{2\tau_0 q_n^2+\frac{Eh^3}{12(1-\nu^2)}\left(1+\frac{\eta_2}{h}\right)q_n^4\right\}. \tag{36}$$

Therefore, the solutions of the resultant forces and moments for the static cylindrical bending are obtained as

$$N^*_{11}=N^*_{21}=0,\qquad M^*_{11}=\frac{Eh^3}{12(1-\nu^2)}\left(1+\frac{\eta_2}{h}\right)U^*_{3K}q_n^2\sin q_n x_1, \tag{37}$$

where U^*_{3K} is given in (36).

It is noted from (36) and (37) that the bending stiffness for the cylindrical bending by including surface effects can be defined by

$$D^*=D_0(1+\eta_2/h), \tag{38}$$

where $D_0=Eh^3/12(1-\nu^2)$ is the bending stiffness of an isotropic material in classical plate theories. For comparison, the bending stiffness for cylindrical bending based on equations in Lim and He (2004) but omitting nonlinear effects is also listed here:

$$D^*_1=D_0[1+(\eta_2+\nu l_1)/h], \tag{39}$$

where l_1 is given in (22). Thus, the non-dimensional difference between different bending modulus are obtained as

$$\frac{D^*-D_0}{D_0}=\frac{\eta_2}{h},\qquad \frac{D^*-D^*_1}{D_0}=-\frac{\nu l_1}{h}. \tag{40}$$

It is seen that the differences are similar as those obtained by Miller and Shenoy (2000), and are inversely proportional to plate thickness h. The parameter η_2 is the ratio between the surface properties and the bulk properties to determine significance of surface effects under cylindrical bending, and is explicitly given by $\eta_2 = [6(1-\nu^2)(\lambda_0+\mu_0+\tau_0) - 2\nu(1-\nu)\tau_0]/E$.

Fig. 1 shows the differences for the properties of materials I and II respectively. For the data of material I, the size effect becomes significant when the thickness of the film is smaller than 10 μm (Fig. 1a), while for data of material II it is significant when the thickness of the film is of the order of 1 nm (Fig. 1b). The results agree with the discussions by Lim and He (2004) for the same problems. It is also noted that the bending stiffness increases for the material I (Fig. 1a), while decreases for the material II (Fig. 1b), when the film thickness is reduced. It shows that surface effects could stiffen or soften material properties (Zhou and Huang, 2004). The significant difference of the thickness order on the influence of the size effects for the materials I and II is due to the surface elastic properties defined for the two materials. It is noted that the surface elastic properties for the material I are approximately 3 order higher than those for the material I, which in turn significantly increase the order of the critical thickness for the material I. Therefore, reliable elastic properties for the surface layer play very important roles to provide reasonable predictions based on the continuum models.

In addition, Fig. 2 also shows the non-dimensional differences of effective bending modulus by the two theories. For the data of material I, the difference is three order smaller than the value shown in Fig. 1a, which means that both theories can provide similar predications. For the data of material II, however, the difference shown in Fig. 2b is only one order smaller than the value shown in Fig. 1b, and should be considered in the calculations. It is because that $(D^* - D_1^*)/D_0 \sim \tau_0/h$, and the surface stress τ_0 is two to three order smaller than corresponding surface material constants λ_0 and μ_0 for material I, and is in same order for material II. Therefore, for surface properties of material with the same order values of τ_0, λ_0 and μ_0, in which the intrinsic material length is not dominated by the surface constants λ_0 and μ_0, more general theories given in the paper should be used.

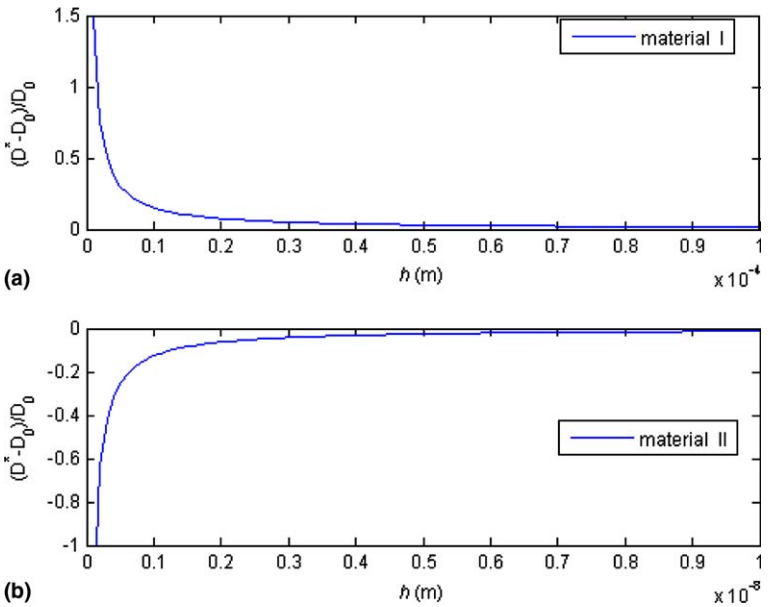

Fig. 1. Non-dimensional difference between plate bending modulus predicted by present size-dependent plate theory and that by classical plate theory: (a) for data of material I and (b) for data of material II.

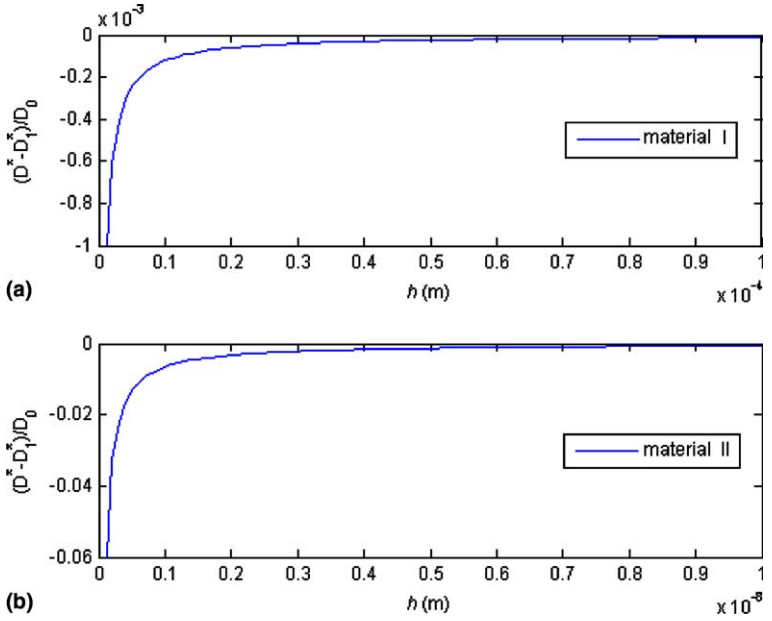

Fig. 2. Non-dimensional difference between plate bending modulus predicted by present plate model and that by Lim and He's (2004) plate model: (a) for data of material I and (b) for data of material II.

By considering $n = 1$, the maximal transverse displacement in (36) can be written as

$$U^*_{3K} = \frac{U_{3K}}{12(1-\nu)(s/\pi)^2 l_1/h + (1+\eta_2/h)}, \qquad U_{3K} = \frac{12(1-\nu^2)h}{E}\left(\frac{s}{\pi}\right)^4 P_3, \tag{41}$$

where $s = l/h$ is span-to-thickness ratio, U_{3K} the maximal transverse displacement without considering surface effects. For constant span-to-thickness ratio $s = 10$, the non-dimensional differences of the transverse displacements are shown in Fig. 3a and b, respectively, for the data of materials I and II. It is seen that size effects tend to be significant when the thickness of the film approach to intrinsic length scales of the materials.

5.1.2. Free vibration

It is seen from (32) that the in-plane and out-of-plane vibrations are uncoupled for the cylindrical vibration. To obtain the frequency of transverse vibration, it is assumed that u^0_3 is of the form

$$u^0_3 = U^*_{3K} \sin q_n x_1 \sin \omega_n t, \tag{42}$$

where ω_n is the nth order frequency of transverse vibration. By substituting (42) into third equation in (32), the frequency ω_n can be obtained as

$$\omega_n^2 = \left[2\tau_0 q_n^2 + \frac{Eh^3}{12(1-\nu^2)}\left(1+\frac{\eta_2}{h}\right)q_n^4\right] \Big/ \left[(I+2\rho_0) + \left(J + \frac{h^2}{6}\frac{3-4\nu}{1-\nu}\rho_0\right)q_n^2\right]. \tag{43}$$

If the surface effects are neglected, Eq. (43) is reduced to the expressions of the frequencies for classical plate theory. The non-dimensional differences between the first order frequencies with and without the surface effects are shown in Fig. 4, where $s = 10$ is taken. The size dependent resonant properties should receive

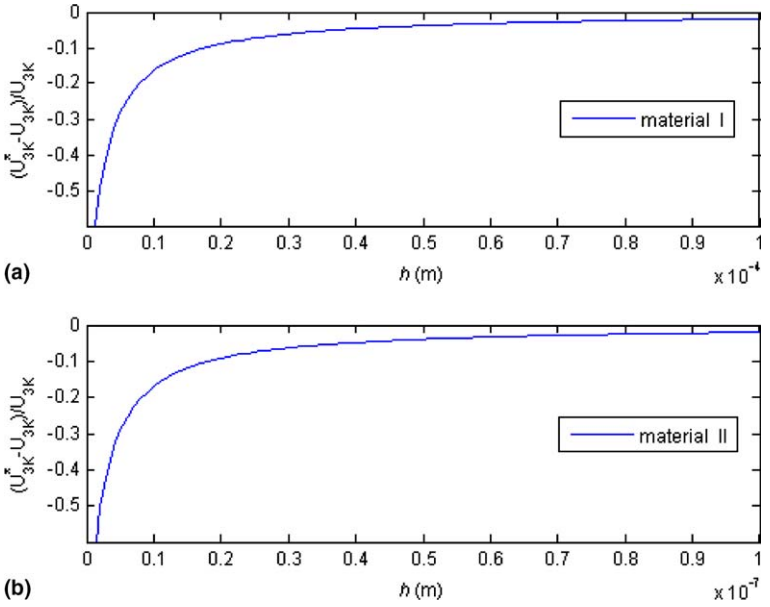

Fig. 3. Non-dimensional difference between deflection predicted by present size-dependent Kirchhoff plate theory and that by classical Kirchhoff plate theory: (a) for data of material I and (b) for data of material II.

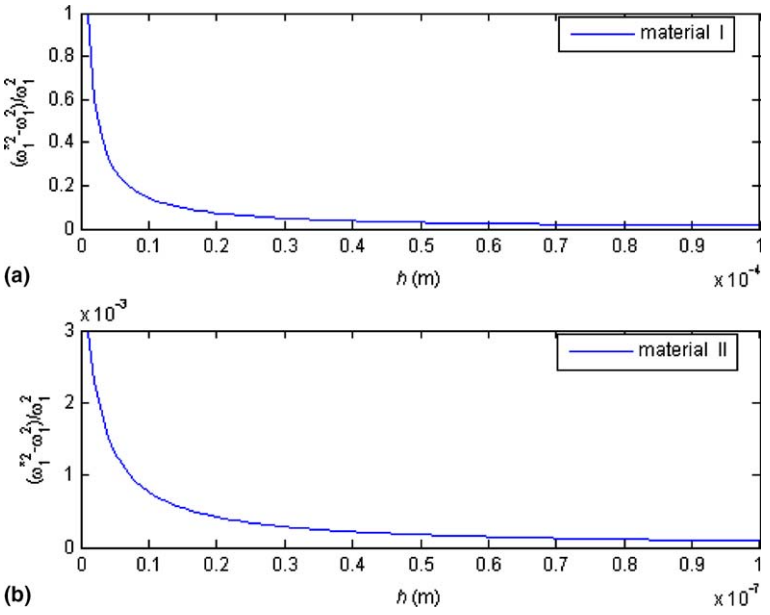

Fig. 4. Non-dimensional difference between the first order frequency predicted by present size-dependent Kirchhoff plate theory and that by classical Kirchhoff plate theory: (a) for data of material I and (b) for data of material II.

special attention in the design of micro/nanoresonant sensors, in which surface effects play a significant role (Lavrik et al., 2004).

5.2. Solutions with Mindlin theory

In Mindlin plate theory, the displacement field for cylindrical bending has the form

$$u_1 = u_1^0 + x_3\psi_1, \qquad u_2 = u_2^0, \qquad u_3 = u_3^0, \tag{44}$$

where $u_i^0 = u_i^0(x_1;t)$ and $\psi_1 = \psi_1(x_1;t)$ rely on x_1 only. The resultant forces and moments (28) for Mindlin plate theory are reduced to

$$\begin{aligned}
N_{11}^* &= 2\tau_0 + \frac{Eh}{1-v^2}\left(1+\frac{\eta_1}{h}\right)u_{1,1}^0,\\
N_{21}^* &= \frac{Eh}{2(1+v)}\left(1+\frac{2l_2}{h}\right)u_{2,1}^0,\\
N_{31}^* &= \frac{Eh}{2(1+v)}\left[\left(1+\frac{2l_1}{h}\right)u_{3,1}^0 + \psi_1\right],\\
M_{11}^* &= \frac{Eh^3}{12(1-v^2)}\left[\left(1+3\frac{\eta_1}{h}\right)\psi_{1,1} + v\frac{l_1}{h}u_{3,11}^0\right] - \frac{vh^2}{6(1-v)}\rho_0\ddot{u}_3^0,
\end{aligned} \tag{45}$$

where η_1 is given in (31), and the equations of motion (29) are reduced to

$$\begin{aligned}
&\frac{Eh}{1-v^2}\left(1+\frac{\eta_1}{h}\right)u_{1,11}^0 + p_1 = (I+2\rho_0)\ddot{u}_1^0, \qquad \frac{Eh}{2(1+v)}\left(1+\frac{2l_2}{h}\right)u_{2,11}^0 + p_2 = (I+2\rho_0)\ddot{u}_2^0,\\
&\frac{Eh}{2(1+v)}\left[\left(1+\frac{2l_1}{h}\right)u_{3,11}^0 + \psi_{1,1}\right] + p_3 = (I+2\rho_0)\ddot{u}_3^0,\\
&\frac{Eh^3}{12(1-v^2)}\left[\left(1+3\frac{\eta_1}{h}\right)\psi_{1,11} + v\frac{l_1}{h}u_{3,111}^0\right] - \frac{Eh}{2(1+v)}[u_{3,1}^0 + \psi_1] + r_1 = \left(J+\frac{h^2}{2}\rho_0\right)\ddot{\psi}_1^+ \frac{h^2 v}{6(1-v)}\rho_0\ddot{u}_{3,1}^0.
\end{aligned} \tag{46}$$

5.2.1. Static bending

Similar to the expressions given in (34), the displacement field satisfying the simply supported edge boundary conditions can be written as

$$u_\alpha^0 = U_{\alpha M}^* \cos q_n x_1, \qquad u_3^0 = U_{3M}^* \sin q_n x_1, \qquad \psi_1 = \Psi_{1M}^* \cos q_n x_1, \tag{47}$$

where q_n is defined in (35), and $U_{\alpha M}^*$, U_{3M}^* and Ψ_{1M}^* indicate maximal values of displacement components under Mindlin theory.

Again assuming that the plate is subjected to sinusoidal loading $p_3 = P_3 \sin q_n x_1$ only, and $p_1 = p_2 = r_1 = 0$. By substituting (47) and nonzero load to (46) and considering static terms only, we have

$$\begin{aligned}
&U_{1M}^* = U_{2M}^* = 0, \qquad \left(1+\frac{2l_1}{h}\right)q_n^2 U_{3M}^* + q_n\Psi_{1M}^* = \frac{2(1+v)}{Eh}P_3,\\
&\left[v\frac{l_1}{h}q_n^3 + \frac{6(1-v)}{h^2}q_n\right]U_{3M}^* + \left[\left(1+3\frac{\eta_1}{h}\right)q_n^2 + \frac{6(1-v)}{h^2}\right]\Psi_{1M}^* = 0,
\end{aligned} \tag{48}$$

which gives solutions for U_{3M}^* and Ψ_{1M}^* as

$$U_{3M}^* = \frac{\Delta_1}{\Delta}, \qquad \Psi_{1M}^* = \frac{\Delta_2}{\Delta}, \tag{49}$$

where

$$\begin{aligned}
\Delta_1 &= -\frac{2(1+\nu)}{Eh}\left[\left(1+3\frac{\eta_1}{h}\right)q_n^2+\frac{6(1-\nu)}{h^2}\right]P_3,\\
\Delta_2 &= \frac{2(1+\nu)}{Eh}\left[\nu\frac{l_1}{h}q_n^3+\frac{6(1-\nu)}{h^2}q_n\right]P_3,\\
\Delta &= -\left[1+\frac{3\eta_1+(2-\nu)l_1}{h}+\frac{6\eta_1 l_1}{h^2}\right]q_n^4-\frac{12(1-\nu)l_1}{h^3}q_n^2.
\end{aligned} \tag{50}$$

Therefore, the solutions of the resultant forces and moments for the static cylindrical bending are obtained as

$$\begin{aligned}
N_{11}^* &= N_{21}^* = 0,\\
N_{31}^* &= \frac{Eh}{2(1+\nu)}\left[\left(1+\frac{2l_1}{h}\right)q_n U_{3M}^* + \Psi_{1M}^*\right]\cos q_n x_1,\\
M_{11}^* &= -\frac{Eh^3}{12(1-\nu^2)}\left[\left(1+3\frac{\eta_1}{h}\right)\Psi_{1M}^* + \nu\frac{l_1}{h}q_n U_{3M}^*\right]q_n \sin q_n x_1,
\end{aligned} \tag{51}$$

where U_{3M}^* and Ψ_{1M}^* are given in (49).

By considering $n=1$ and $s=l/h$, the maximal displacement and rotation components in (49) can be written as

$$\begin{aligned}
U_{3M}^* &= \frac{1+3\eta_1/h+6(1-\nu)(s/\pi)^2}{1+[3\eta_1+(2-\nu)l_1]/h+6\eta_1 l_1/h^2+12(1-\nu)(s/\pi)^2 l_1/h}\frac{2(1+\nu)(s/\pi)^2 h}{E}P_3,\\
\Psi_{1M}^* &= -\frac{\nu l_1/h+6(1-\nu)(s/\pi)^2}{1+[3\eta_1+(2-\nu)l_1]/h+6\eta_1 l_1/h^2+12(1-\nu)(s/\pi)^2 l_1/h}\frac{2(1+\nu)s/\pi}{E}P_3.
\end{aligned} \tag{52}$$

If the surface effects are neglected, the about results are reduced to the corresponding expressions in classical Mindlin plate theory:

$$U_{3M} = \frac{2(1+\nu)(s/\pi)^2[1+6(1-\nu)(s/\pi)^2]h}{E}P_3, \qquad \Psi_{1M} = -\frac{12(1-\nu^2)(s/\pi)^3}{E}P_3. \tag{53}$$

For constant span-to-thickness ratio $s=10$, the non-dimensional differences between the components computed, respectively, by including and without considering the surface effects are shown in Fig. 5 for the data of materials I and II. It is seen that the differences for the transverse displacement and the rotation component are in similar ranges when the thickness of the film approach to its intrinsic length scales.

In Fig. 6, the ratio of the transverse displacement components between Kirchhoff and Mindlin plate theories are plotted. In classical plate models, thickness shear strains are not considered in Kirchhoff theory, but are introduced in Mindlin theory. Therefore, the behavior of a plates based on Kirchhoff plate theory is generally stiffer than that based on Mindlin plate theory. If the surface effects are not considered, the transverse deflection ratio U_{3K}/U_{3M} is always smaller than one. However, it is interesting to note from Fig. 6 that if the surface effects are considered, the ratio U_{3K}^*/U_{3M}^* tends to increase when the film thickness is reduced.

5.2.2. Free vibration

It is seen from (46) that the in-plane and out-of-plane vibrations are still uncoupled for the cylindrical vibration in Mindlin plate theory. To obtain the frequency of transverse vibration, it is assumed that u_3^0 and ψ_1 have the form

$$u_3^0 = U_{3M}^* \sin q_n x_1 \sin \omega_n t, \qquad \psi_1 = \Psi_{1M}^* \cos q_n x_1 \sin \omega_n t. \tag{54}$$

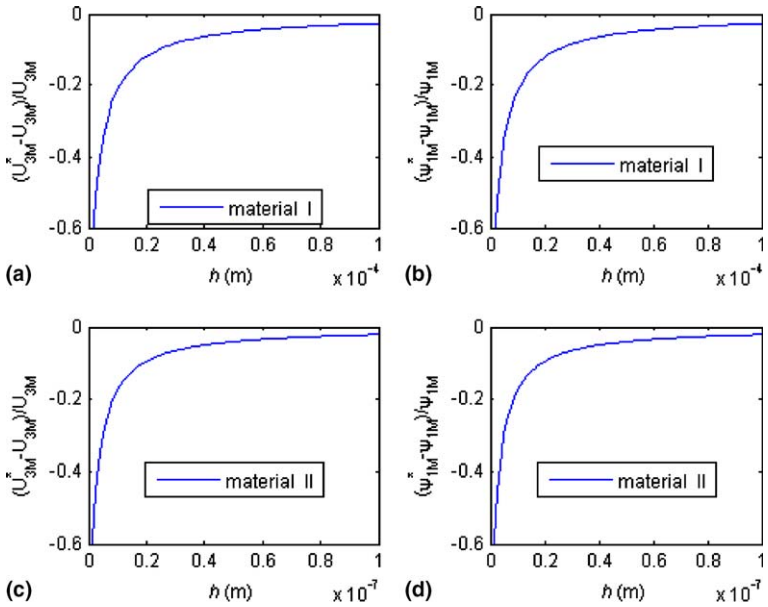

Fig. 5. Non-dimensional differences of deflection and rotation predicted, respectively, by present size-dependent Mindlin plate theory and classical Mindlin plate theory: (a) difference of deflection for data of material I, (b) difference of rotation for data of material I, (c) difference of deflection for data of material II, and (d) difference of rotation for data of material II.

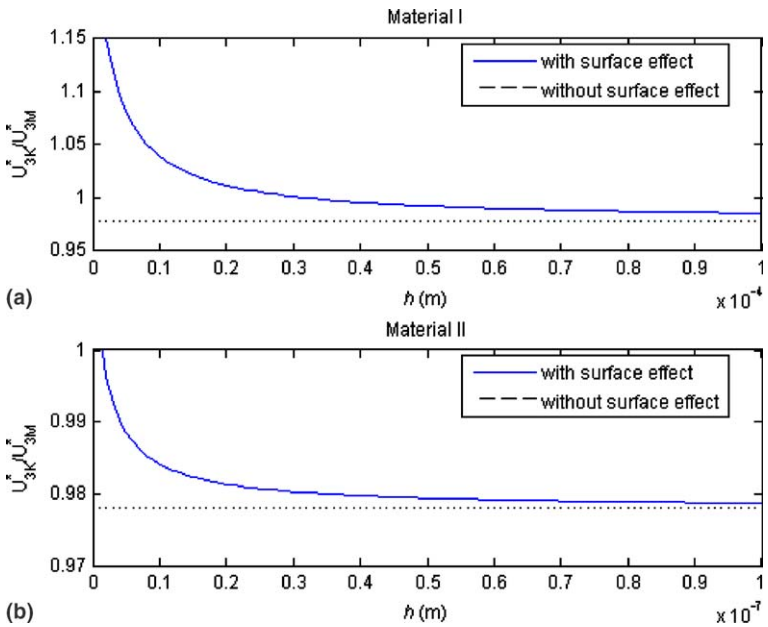

Fig. 6. Ratio of deflections predicted by size-dependent Kirchhoff and Mindlin plate theories, respectively: (a) for data of material I and (b) for data of material II.

By substituting (54) into last two equations in (22), we have

$$\begin{aligned}
&\frac{Eh}{2(1+\nu)}\left[\left(1+\frac{2l_1}{h}\right)q_n^2U_{3M}^*+q_n\Psi_{1M}^*\right]=(I+2\rho_0)U_{3M}^*\omega_n^2,\\
&\frac{Eh^3}{12(1-\nu^2)}\left[\left(1+3\frac{\eta_1}{h}\right)q_n^2\Psi_{1M}^*+\nu\frac{l_1}{h}q_n^3U_{3M}^*\right]+\frac{Eh}{2(1+\nu)}[q_nU_{3M}^*+\Psi_{1M}^*]\\
&\quad=\left[\left(J+\frac{h^2}{2}\rho_0\right)\Psi_{1M}^*+\frac{h^2\nu}{6(1-\nu)}\rho_0q_nU_{3M}^*\right]\omega_n^2,
\end{aligned}\tag{55}$$

which can be further simplified as

$$\begin{aligned}
&(A_{11}-B_{11}\omega_n^2)U_{3M}^*+A_{12}\Psi_{1M}^*=0,\\
&(A_{21}-B_{21}\omega_n^2)U_{3M}^*+(A_{22}-B_{22}\omega_n^2)\Psi_{1M}^*=0,
\end{aligned}\tag{56}$$

where

$$\begin{aligned}
&A_{11}=\left(1+\frac{2l_1}{h}\right)q_n^2,\qquad A_{12}=q_n,\qquad A_{21}=\nu\frac{l_1}{h}q_n^3+\frac{6(1-\nu)}{h^2}q_n,\\
&A_{22}=\left(1+3\frac{\eta_1}{h}\right)q_n^2+\frac{6(1-\nu)}{h^2},\qquad B_{11}=\frac{2(1+\nu)}{Eh}(I+2\rho_0),\\
&B_{21}=\frac{2\nu(1+\nu)}{Eh}\rho_0q_n,\qquad B_{22}=\frac{12(1-\nu^2)}{Eh^3}\left(J+\frac{h^2}{2}\rho_0\right).
\end{aligned}\tag{57}$$

From (56), non-trivial solutions for U_{3M}^* and Ψ_{1M}^* require that

$$C_1\omega_n^4+C_2\omega_n^2+C_3=0,\tag{58}$$

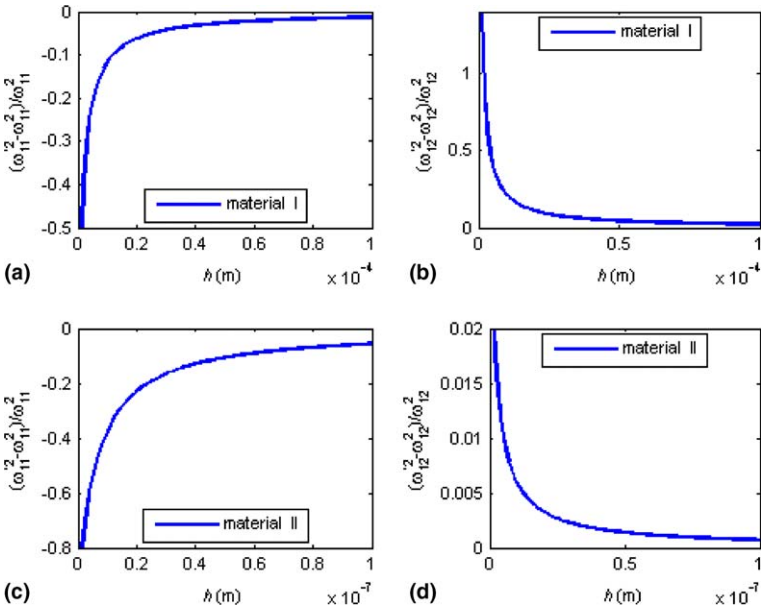

Fig. 7. Non-dimensional differences between frequencies predicted by present size-dependent Mindlin plate theory and those by classical Mindlin plate theory: (a) and (b) for data of material I, (c) and (d) for data of material II.

with

$$C_1 = B_{11}B_{22}, \qquad C_2 = A_{12}B_{21} - A_{11}B_{22} - B_{11}A_{22}, \qquad C_3 = A_{11}A_{22} - A_{12}A_{21}. \tag{59}$$

Therefore, with each n, we obtain two frequencies. One is the frequency for the transverse vibration, and the other is the frequency for the thickness shear vibration, which are given by

$$\omega_{n1}^{*2} = \frac{-C_2 + \sqrt{C_2^2 - 4C_1C_3}}{2C_1}, \qquad \omega_{n2}^{*2} = \frac{-C_2 - \sqrt{C_2^2 - 4C_1C_3}}{2C_1}. \tag{60}$$

The non-dimensional differences between the frequencies with and without the surface effects are shown in Fig. 7 for $s = 10$ and $n = 1$. It also shows that the size effects tend to be significant when the thickness of the film reaches its intrinsic length scales.

6. Concluding remarks

A thin plate model including the surface effects which can be used for size-dependent static and dynamic analysis of plate-like thin film structures has been proposed. This model is a modification and generalization of the thin plate theory developed by Lim and He (2004). The model is derived based on linear elasticity theory for simplicity, but can also be extended to the problems with nonlinear deformations as treated in Lim and He (2004). By comparing with the relations given in Lim and He (2004) but omitting the nonlinear effects, the Kirchhoff plate theory derived in this paper have some additional terms. The coefficients of these terms relate to the surface stress τ_0 and surface density ρ_0 only for isotropic material properties considered. Therefore, the differences of the results obtained by the two models rely on the magnitudes of these two surface properties as discussed in Fig. 2. The numerical examples show that the size effects tend to be significant when the thicknesses of the plate-like thin film structures approach to its intrinsic length scales of the materials, which is generally found to be in agreement with results from experiments and atomistic simulations. To predict the overall static and dynamic properties of a plate-like thin film structure based on the continuum model, reliable material constants of its bulk and surface materials should be known. Therefore, precise measurement technique or efficient atomistic computational means are required to extract the constants.

References

Cammarate, R.C., Sieradzki, K., 1989. Effects of surface stress on the elastic moduli of thin films and superlattices. Phys. Rev. Lett. 62, 2005–2008.

Cuenot, S., Fretigny, C., Demoustier-Champagne, S., Nysten, B., 2004. Surface tension effect on the mechanical properties of nanomaterials measured by atomic force microscopy. Phys. Rev. B 69, 165410.

Evoy, S., Carr, D.W., Sekaric, L., Olkhovets, A., Parpia, J.M., Craighead, H.G., 1999. Nanofabrication and electrostatic operation of single-crystal silicon paddle oscillations. J. Appl. Phys. 86, 6072–6077.

Gurtin, M.E., Murdoch, A.I., 1975a. A continuum theory of elastic material surfaces. Arch. Rat. Mech. Anal. 57, 291–323.

Gurtin, M.E., Murdoch, A.I., 1975b. Addenda to our paper: a continuum theory of elastic material surfaces. Arch. Rat. Mech. Anal. 59, 389–390.

Gurtin, M.E., Murdoch, A.I., 1978. Surface stress in solids. Int. J. Solids Struct. 14, 431–440.

He, L.H., Lim, C.W., Wu, B.S., 2004. A continuum model for size-dependent deformation of elastic films of nano-scale thickness. Int. J. Solids Struct. 41, 847–857.

Ibach, H., 1997. The role of surface stress in reconstruction, epitaxial growth and stabilization of mesoscopic structures. Surf. Sci. Rep. 29, 193–263.

Lavrik, N.V., Sepaniak, M.J., Datskos, P.G., 2004. Cantilever transducers as a platform for chemical and biological sensors. Rev. Sci. Instrum. 75, 2229–2253.

Lim, C.W., He, L.H., 2004. Size-dependent nonlinear response of thin elastic films with nano-scale thickness. Int. J. Mech. Sci. 46, 1715–1726.
Miller, R.E., Shenoy, V.B., 2000. Size-dependent elastic properties of nanosized structural elements. Nanotechnology 11, 139–147.
Muller, P., Saul, A., 2004. Elastic effects on surface physics. Surf. Sci. Rep. 54, 157–258.
Murdoch, A.I., 1976. The propation of surface waves in bodies with material boundaries. J. Mech. Phys. Solids 24, 137–146.
Sharma, P., Ganti, S., 2004. Size-dependent Eshelby's tensor for embedded nano-inclusions incorporating surface/interface energies. J. Appl. Mech. 71, 663–671.
Sharma, P., Ganti, S., Bhate, N., 2003. Effect of surfaces on the size-dependent elastic state of nano-inhomogeneities. Appl. Phys. Lett. 82, 535–537.
Shenoy, V.B., 2002. Size-dependent rigidities of nanosized torsional elements. Int. J. Solids Struct. 39, 4039–4052.
Sun, C.T., Zhang, H., 2003. Size-dependent elastic moduli of platelike nanomaterials. J. Appl. Phys. 93, 1212–1218.
Wong, E.W., Sheehan, P.E., Lieber, C.M., 1997. Nanobeam mechanics: elasticity, strength, and toughness of nanorods and nanotubes. Science 277, 1971–1975.
Zhang, H., Sun, C.T., 2004. Nanoplate model for platelike nanomaterials. AIAA J. 42, 2002–2009.
Zhou, L.G., Huang, H., 2004. Are surface elastically softer or stiffer? Appl. Phys. Lett. 84, 1940–1942.